

Shell-model configuration-interaction description of quadrupole collectivity in Te isotopes

Chong Qi*

Department of Physics, KTH Royal Institute of Technology, 10691 Stockholm, Sweden

(Received 7 July 2016; revised manuscript received 10 August 2016; published 8 September 2016)

Systematic calculations on the spectroscopy and transition properties of even-even Te isotopes are carried out by using the large-scale shell-model configuration-interaction approach with a realistic interaction. These nuclei are of particular interest since their yrast spectra show a vibrational-like equally spaced pattern whereas the few known $E2$ transitions show rotational-like behavior. This cannot be explained by available collective models. My calculations reproduce well the equally spaced spectra of those isotopes as well as the constant behavior for the $B(E2)$ values of ^{114}Te . The calculated $B(E2)$ values of neutron-deficient and heavier Te isotopes show contrasting different behaviors along the yrast line. The $B(E2)$ of light isotopes can exhibit a nearly constant behavior up to high spins. It is shown that this is related to the enhanced neutron-proton correlation when approaching $N = 50$.

DOI: [10.1103/PhysRevC.94.034310](https://doi.org/10.1103/PhysRevC.94.034310)**I. INTRODUCTION**

The advent of large-scale radioactive beam facilities and new detection technologies have enabled the study of the spectroscopy and transition properties of $N \sim Z$ nuclei just above the presumed doubly magic nucleus ^{100}Sn [1]. Several unexpected phenomena have recently been observed: Large $B(E2; 2_1^+ \rightarrow 0_1^+)$ values of neutron deficient semimagic Sn isotopes have triggered extensive experimental [2–6,6–12] and theoretical [13–21] activities, in particular regarding the fundamental roles played by core excitations and the nuclear pairing correlation (or seniority coupling). The study of transition rates in isotopic chains just above $Z = 50$ may provide further information on the role of core excitations [22,23]. The limited number of valence protons and neutrons are not expected to induce any significant quadrupole correlation in this region [24–27]. The low-lying collective excitations of Te isotopes were discussed in terms of quadrupole vibrations [24,28] in relation to the fact that the even-even isotopes between $N = 56$ and 70 show regular equally spaced yrast spectra (cf., Fig. 1 in Ref. [24]). If that is the case, the Te isotopes will provide an ideal ground to explore the nature of the elusive nuclear vibration and the residual interactions leading to that collectivity. However, the available $E2$ transition strengths along the yrast line in $^{114,120-124}\text{Te}$ show a rotational-like behavior, which cannot be reproduced by collective models or the interacting boson model [29,30]. It indicates that the Te isotopes may not be dominated by vibration but by other kinds of correlation. Another intriguing phenomenon is the nearly constant behavior of the energies of the 2^+ and 4^+ states in Te and Xe isotopes and their ratios when approaching $N = 50$, in contrast to the decreasing behavior when approaching $N = 82$ [24]. This was analyzed in Ref. [31] based on the quasiparticle random phase approximation approach where a competition between the quadrupole-quadrupole correlation and neutron-proton pairing correlation was suggested.

An enhanced interplay between neutrons and protons is expected in the ^{100}Sn region since the protons and neutrons partially occupy the same quantum orbitals near the Fermi level [24,31–33]. In relation to that, there has also been a long effort searching for superallowed α decays from those $N \sim Z$ isotopes [34,35]. The region is also expected to be the endpoint of the astrophysical rapid proton capture (rp) process [36,37]. The octupole correlation may also play a role here (the coupling between the $0h_{11/2}$ and $1d_{5/2}$ orbitals) [26,38,39]. Still, compared to tin, the experimental information is less abundant in the isotopic chain of tellurium where little was known experimentally below the neutron midshell until recently. Much more work is needed and further measurements are underway in order to map out the ordering and nature of single-particle states and two-body effective interactions in the region [40,41].

In this work I present systematic large-scale calculations on the spectroscopy and transition properties of even-even Te isotopes. The large-scale shell model, which takes into account all degrees of freedom within a given model space, is an ideal approach to study competition between collective and single-particle degrees of freedom. It is however a challenge, especially in the midshell, due to the huge dimension of the problem (cf. Fig. 1 in Ref. [21]). I have carried out systematic calculations on the $B(E2; 2_1^+ \rightarrow 0_1^+)$ values of even-even Te isotopes [22,23]. The results are, however, rather sensitive to the truncation imposed. One is now able to extend significantly my full shell-model calculations to all low-lying states of all Te isotopes with further optimization of the shell-model algorithm. A full shell-model calculation for the spectroscopy of ^{104}Te was performed in Ref. [1]. A schematic calculation for ^{106}Te in the $1d_{5/2}0g_{7/2}$ subspace was presented in Ref. [24]. Systematic calculations on the Sn and Sb isotopes were given in Refs. [20,21] and Ref. [42], respectively. In Ref. [27], the possible onset of vibrational collectivity in Te isotopes was discussed within an effective field theory framework. In Ref. [25], the quadrupole collectivity of light Xe isotopes was studied within the shell-model approach in a truncated model space. Unlike Te, the Xe isotopes show rather rotational-like spectra with increasing space between neighboring yrast levels.

*chongq@kth.se

II. MODEL

I consider the neutron and proton orbitals between the shell closures N (and Z) = 50 and 82, comprising $0g_{7/2}$, $1d_{5/2}$, $1d_{3/2}$, $2s_{1/2}$, and $0h_{11/2}$ and assume ^{100}Sn as the inert core. The robustness of the $N = Z = 50$ shell closures, which has fundamental influence on my understanding of the structure of nuclei in this region, is supported by recent measurements [9,20,22,23,43]. One also assumes isospin symmetry in the effective Hamiltonian written as

$$H = \sum_{\alpha} \varepsilon_{\alpha} \hat{N}_{\alpha} + \frac{1}{4} \sum_{\alpha\beta\delta\gamma JT} \langle j_{\alpha} j_{\beta} | V | j_{\gamma} j_{\delta} \rangle_{JT} A_{JT; j_{\alpha} j_{\beta}}^{\dagger} A_{JT; j_{\gamma} j_{\delta}}, \quad (1)$$

where $\alpha = \{nljt\}$ denote the single-particle orbitals and ε_{α} stand for the corresponding single-particle energies. $\hat{N}_{\alpha} = \sum_{j_z, t_z} a_{\alpha, j_z, t_z}^{\dagger} a_{\alpha, j_z, t_z}$ is the particle number operator. $\langle j_{\alpha} j_{\beta} | V | j_{\gamma} j_{\delta} \rangle_{JT}$ are the two-body matrix elements coupled to good spin J and isospin T . A_{JT} (A_{JT}^{\dagger}) is the fermion pair annihilation (creation) operator. The nearly degenerate neutron single-particle states $d_{5/2}$ and $g_{7/2}$ orbitals in ^{101}Sn were observed by studying the α decay $^{105}\text{Te} \rightarrow ^{101}\text{Sn}$ [34,35,44,45]. Based on the assumption that the ground state of ^{105}Te has spin parity $5/2^{+}$, the $g_{7/2}$ orbital was suggested to be the ground state of ^{101}Sn instead of $d_{5/2}$. The excitation energy of the $1d_{5/2}$ is taken as $\varepsilon(1d_{5/2}) = 0.172$ MeV. The energies of other states have not been measured yet. They are adjusted to fit the experimental binding energies of tin isotopes. The starting point of my calculation is the realistic CD-Bonn nucleon-nucleon potential [46]. The interaction was renormalized using the perturbative G -matrix approach to take into account the core-polarization effects [47]. The $T = 1$ part of the monopole interaction was optimized by fitting to the low-lying states in Sn isotopes [21]. Further optimization of the $T = 0$ part of the interaction is also underway which, however, is still a very challenging task. My calculations show that the present effective Hamiltonian are already pretty successful in describing the structure and transition properties of Sb, Te, I, Xe, and Cs isotopes as well as heavy nuclei near $N = 82$ in this region.

The Te isotopic chain is the heaviest and longest chain that can be described by the nuclear shell model. The dimension for the midshell ^{118}Te reaches 10^{10} for which the diagonalization is still a very challenging numeric task. In my previous calculations for the $B(E2; 2_1^{+} \rightarrow 0_1^{+})$ of midshell Te isotopes [22], I restricted a maximum of four neutrons that can be excited from below the Fermi surface to the neutron $h_{11/2}$ subshell and excluded proton excitation to $h_{11/2}$ due to limited computation power, which, as one understands now, is a rather severe truncation. The model space was further extended to allow at most eight particles to the $h_{11/2}$ subshell in Ref. [23], where the $B(E2; 2_1^{+} \rightarrow 0_1^{+})$ values show a much smoother parabolic behavior as a function of N . Full shell-model calculations are performed for all nuclei in the present work. All shell-model calculations are carried out within the M scheme where states with $M = I$ are considered. Diagonalizations are carried out with a parallel shell-model program that I developed [48] and with a slightly modified version of the code KSHELL [49]. All calculations are performed on the supercomputers Beskow and Tegnér at PDC Center for High Performance Computing at the KTH Royal Institute of Technology in Stockholm, Sweden.

III. CALCULATIONS

To test the validity of the effective interaction, I have performed systematic calculations on the yrast spectra of isotopes $^{104-132}\text{Te}$. The results for $^{104-118}\text{Te}$ are plotted in Fig. 1 in comparison with available experimental data [50]. An overall good agreement between theory and experiment is obtained. A noticeable difference is seen in the excitation energies of the 12^{+} states in $^{112,114}\text{Te}$ and the $I \geq 6$ states in ^{106}Te . All isotopes plotted in the figure show rather regular and vibrational-like spectra up to 12^{+} except ^{106}Te . For that nucleus, the calculated spectrum still shows an equally spaced pattern. However, a smaller gap between 6_1^{+} and 4_1^{+} states is expected from recent measurement but the spin-parity assignments for those states are still tentative. The equally spaced pattern breaks down in isotopes heavier than ^{126}Te where a gradual depression of the excitation energies of the 6^{+} states is seen.

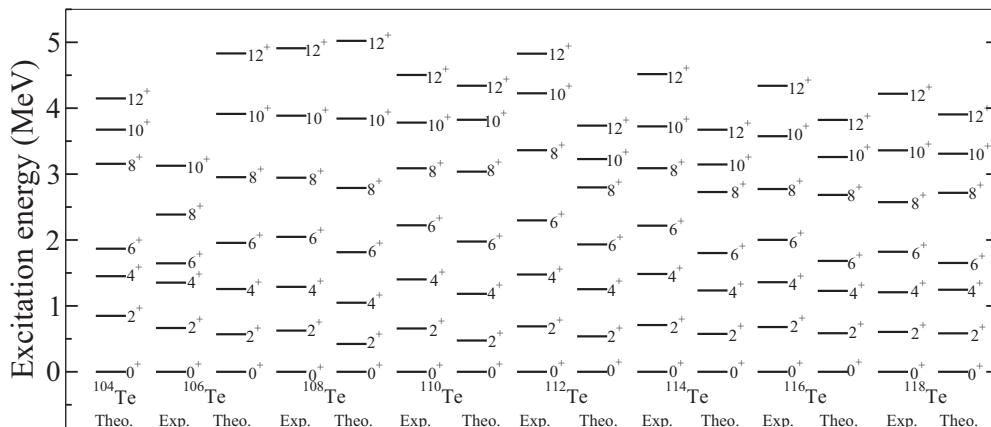


FIG. 1. Comparison between theory and experiment for the yrast spectra of the Te isotopic chain.

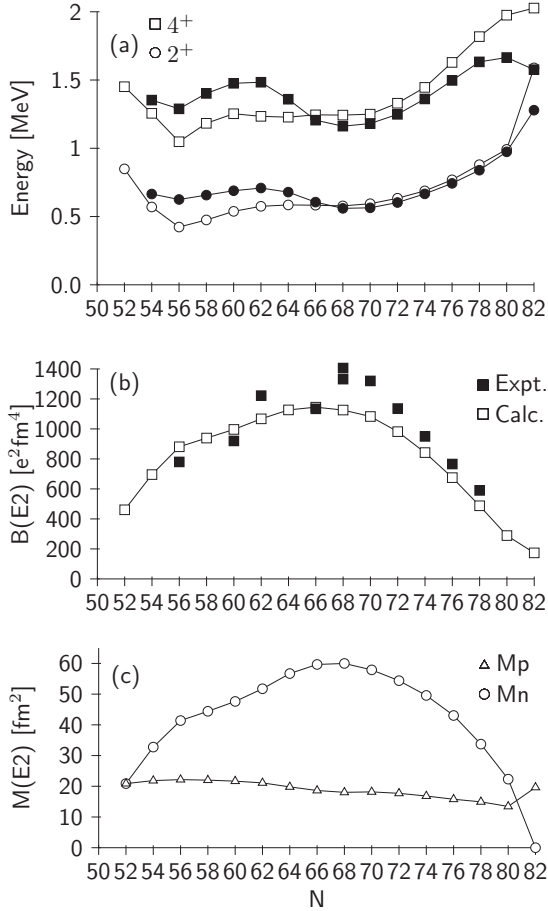


FIG. 2. Comparison between theory and experiment for the energies of the 2^+ and 4^+ yrast states (upper) and the $B(E2; 2_1^+ \rightarrow 0_1^+)$ values (middle) for the Te isotopic chain. The open circles and open triangles in the lower panel correspond to the neutron and proton matrix elements, M_n and M_p , respectively.

A closer comparison between experiment and calculation on the excitation energies of the yrast 2^+ and 4^+ states are plotted in Fig. 2 as a function of neutron number for all even-even Te isotopes. In the lower panel of the figure, the calculated $B(E2; 2_1^+ \rightarrow 0_1^+)$ in tellurium isotopes are compared to the most recent experimental data [22,23,50]. The $B(E2)$ value is calculated as $B(E2; J_i \rightarrow J_f) = |e_p M_p + e_n M_n|^2 / (2J_i + 1)$ where M_p and M_n are the proton and neutron matrix elements. One takes effective charge values $e_p = 1.5e$ and $e_n = 0.8e$ as were employed in Refs. [22,23]. The isospin dependence of the effective charges is not considered here, which is not expected to have large influence on the trend. The model prediction agrees rather well with available data. The largest deviations are seen in isotopes $^{120,122}\text{Te}$. A recent measurement gave a value smaller than the adapted one in the former case. In the lower panel of figure I also plotted the neutron and proton matrix elements, M_n and M_p , which represent the amount of neutron and proton excitations in the wave functions. As can be seen from the figure, the parabolic behavior of the $B(E2)$ values, which looks similar to that of Sn isotopes, follows closely the evolution pattern of M_n . This is related to the fact

that the proton matrix elements M_p show a rather smooth and slightly decreasing behavior as the neutron number increases. An other interesting aspect one notices is that both M_p and M_n show a slight enhancement when approaching $N = Z$: M_p values for isotopes below $N = 56$ are slightly larger than those above. Meanwhile, the neutron matrix elements M_n for $N = 52-58$ deviate from the general decreasing behavior seen from those for $N = 60-66$. As will be discussed below, this could be related to the enhanced neutron-proton correlation in those neutron-deficient nuclei.

As mentioned earlier, the shell-model calculations for midshell Te isotopes, in particular ^{118}Te , are quite sensitive to the filling of both the proton and neutron $h_{11/2}$ subshells. Both the proton and neutron transition matrix elements are enhanced when one goes from a small model space calculation with restricted number of particles in $h_{11/2}$ to the full shell-model calculation.

The regularly spaced level spectra in midshell Te isotopes have been expected to be associated with a collective vibrational motion. For a spectrum corresponding to a vibrator, there should be collective $E2$ transitions between states differing by one phonon. The transition strengths should be linearly proportional to the spin of the initial states, i.e., one has $B(E2, 4_1^+ \rightarrow 2_1^+) / B(E2, 2_1^+ \rightarrow 0_1^+) = 2$ in the harmonic vibrator model. Unfortunately, there are very few data available for $B(E2)$ values in states beyond 2_1^+ . As shown in Ref. [29], the measured $B(E2)$ values along the yrast line in ^{114}Te show a rather constant behavior up to $I = 8$, which looks more like a rotor and is in contradiction with that for a vibrator. My shell-model calculations for those $E2$ transitions are shown in Fig. 3, which indeed exhibit a rather constant behavior up to higher spins. Moreover, my calculations show that both the proton and neutron matrix elements, M_p and M_n , remain roughly the same along the yrast line.

As can be seen Fig. 3, the ratio $B(E2, 4_1^+ \rightarrow 2_1^+) / B(E2, 2_1^+ \rightarrow 0_1^+)$ for ^{114}Te is measured to be even slightly smaller than 1. This is not seen in the theory. The ratio is calculated to be $B(E2, 4_1^+ \rightarrow 2_1^+) / B(E2, 2_1^+ \rightarrow 0_1^+) = 1.38$ which actually agrees well with the prediction for a rotor. As discussed in Refs. [51,52], it happens rarely in open-shell nuclei that one has $B(E2, 4_1^+ \rightarrow 2_1^+) / B(E2, 2_1^+ \rightarrow 0_1^+) < 1$. The reason why the ratio for ^{114}Te is observed to be so small is still not clear.

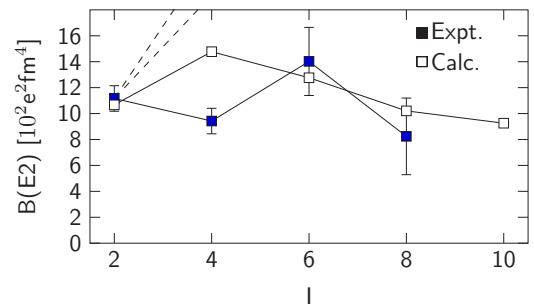


FIG. 3. Comparison between theory and experiment [29] for $B(E2; I_1^+ \rightarrow (I-2)_1^+)$ values in ^{114}Te along the yrast line. The dashed lines correspond to the predictions of collective models [29].

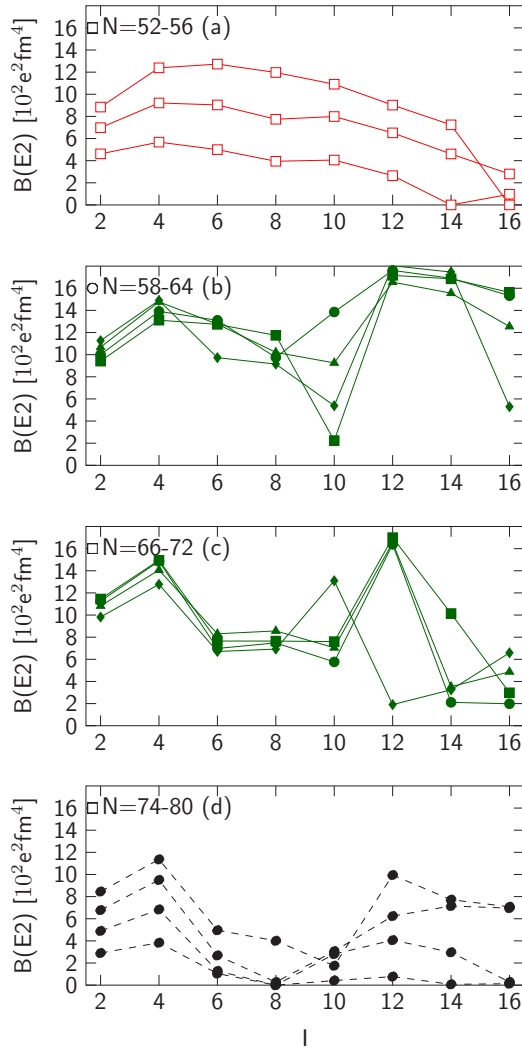


FIG. 4. Calculated $B[E2; I_1^+ \rightarrow (I-2)_1^+]$ values along the yrast line for even-even Te isotopes.

In Ref. [30], the ratios $B(E2, 4_1^+ \rightarrow 2_1^+)/B(E2, 2_1^+ \rightarrow 0_1^+)$ for isotopes $^{120-124}\text{Te}$ are measured to be 1.640, 1.500, and 1.162, respectively. The ratios calculated from the shell-model $B(E2)$ values are 1.322, 1.299, and 1.301, respectively, for the above three nuclei, which agree reasonably with experimental data.

In Fig. 4 I plotted the calculated $B(E2)$ values for the yrast states of all even-even Te isotopes between $N = 52$ and 80. As can be seen from the upper panel of the figure, the $B(E2)$ values for the yrast states of $^{104-108}\text{Te}$, which are at the beginning of the shell, remain roughly constant up to spin $I = 12$ and decrease significantly around $I = 16$, which indicates that the collectivity has collapsed there. On the other hand, as shown in the lower panel of the figure, the results for the isotopes $^{126-132}\text{Te}$ at the end of the shell show a very different behavior: The $B(E2)$ values decrease dramatically after $I = 4$, which reach practically zero value for states up to $I = 10$ in all nuclei except ^{128}Te . The results for the groups $N = 58-64$ and $N = 66-72$ are shown in the middle panels of Fig. 4. In the former group, the $B(E2)$ values show a rather

constant behavior up to $I = 8$. The results for $I = 10$ diverge in relation to the fact that several low-lying 10^+ states are predicted for those nuclei by the shell-model calculations and, in cases like ^{110}Te shown in the panel, it is the second 10^+ state that is connected to the yrast 8^+ state with strong $E2$ transition. As a result, the $B(E2, 10_1^+ \rightarrow 8_1^+)$ value vanishes. In the latter group, the $B(E2)$ values also show a large decrease after $I = 4$ but to an extent that is much less than those in the fourth group, $^{126-132}\text{Te}$.

To understand the behavior of the calculated $B(E2)$ values seen in Fig. 4, one notices that the ratio E_{4^+}/E_{2^+} is roughly equal to 2 for all known Te isotopes below $N = 78$. But it decreases rapidly to around 1.2 in the semimagic ^{134}Te . Moreover, the ratio E_{6^+}/E_{2^+} starts to decrease already at $N = 72$, resulting in senioritylike spectra. The seniority quantum number refers to the number of particles that are not paired to $J = 0$. It is known that, for systems involving the same kind of particles, the low-lying states can be well described within the seniority scheme [53]. This is related to the fact that the $T = 1$ two-body matrix elements are dominated by monopole pairing interactions with $J = 0$. The seniority coupling may be broken by the neutron-proton correlation if both protons and neutrons are present. This indeed happens in the most neutron deficient Te isotopes close to $N = Z$, where the valence neutrons and protons are expected to occupy identical $g_{7/2}$ and $d_{5/2}$ orbitals and the neutron-proton correlation is expected to be strong. As a result, both the spectra and $E2$ transition properties show rather regular collective behaviors. On the other hand, for nuclei $^{126-132}\text{Te}$ at the other end of the shell, the normal seniority coupling may prevail since the neutron-proton correlation involves particles in different shells and is much weaker. As a result, the energy gap between 6^+ and 4^+ as well as the $E2$ transition between the two states reduce significantly (e.g., $E2$ transitions between states with the same seniority are disfavored). The groups $N = 58-64$ and $N = 66-72$ fall between the above two cases.

If the dimension is not too large, it is possible to project the wave function as a coupling of the proton group and neutron group with good angular momenta in the form $|\phi_\pi^p(J_\pi) \otimes \phi_n^n(J_n)\rangle$ where J_π and J_n denote the angular momenta of the proton group and neutron group (see, e.g., [54,55]). The ground state for an even-even nucleus will be represented by a single configuration with $J_\pi = J_n = 0$ if there is no neutron-proton correlation. The neutron-proton interaction induces contributions from configurations with higher angular momenta for the protons and neutrons as well as higher-lying configurations with the same angular momenta. It is seen that, as expected, the ^{104}Te ground state shows a high mixture of many components, among which one has 47% with $J_\pi = J_n = 0$, 30% with $J_\pi = J_n = 2$, 12.5% with $J_\pi = J_n = 4$, and 6.7% with $J_\pi = J_n = 6$. For ^{106}Te ground state the results are 41.7% with $J_\pi = J_n = 0$, 42% with $J_\pi = J_n = 2$, 11.9% with $J_\pi = J_n = 4$. For ^{108}Te ground state the contribution from $J_\pi = J_n = 0$ decreases further to 36.3% while the contribution from $J_\pi = J_n = 2$ increases to 46.6%. The wave functions for other low-lying states show a similar complex structure. On the other hand, the wave functions for the low-lying states of the isotopes $^{126-132}\text{Te}$ show a much simpler picture and are dominated by either

neutron or proton excitations in many cases. The contributions from $J_\pi = J_\nu = 0$ components are 65.2%, 74.4%, and 85.5% for isotopes $^{128-132}\text{Te}$. The 2_1^+ state in ^{132}Te is dominated by $|\phi_\pi^p(J_\pi = 2) \otimes \phi_\nu^n(J_\nu = 0)\rangle$ whereas the 6_1^+ state is dominated by the proton excitation $|\phi_\pi^p(J_\pi = 0) \otimes \phi_\nu^n(J_\nu = 6)\rangle$ instead. The low-lying states for $^{128,130}\text{Te}$ show a similar result. It may be interesting to mention that a similar picture with rotational-like $B(E2)$ transitions and vibrational-like spectrum is also predicted for $N = Z$ nuclei like ^{92}Pd [54] in relation to the quest for the possible existence of neutron-proton pairing in $N \sim Z$ nuclei for which there is still no conclusive evidence after long and extensive studies (see recent discussions in Refs. [54–61]).

IV. SUMMARY

To summarize, I have performed systematic calculations on the spectroscopy and transition properties of Te isotopes within the large-scale configuration-interaction shell-model approach. A monopole-optimized realistic interaction is used. The calculations reproduce well the excitation energies of the low-lying states as well as the regular and vibrational-like behavior of the yrast spectra of $^{108-130}\text{Te}$ (Fig. 1). The energies of the first 2^+ and 4^+ states as well as their ratios show rather a constant behavior when approaching $N = 50$ in relation to the enhanced neutron-proton correlation (Fig. 2). On the other hand, a squeezed gap between the 6_1^+ and 4_1^+ states is expected when approaching $N = 82$, resulting in a senioritylike spectra. Those structure changes are also reflected

in the calculated and available experimental $E2$ transition strengths.

The calculated $B(E2; 2_1^+ \rightarrow 0_1^+)$ show a parabolic behavior as a function of N . That pattern is mostly determined by the contribution from the neutron excitation which reaches its maximum at the midshell. A slight enhancement is seen in both the proton and neutron excitations when approaching the $N = Z$ line. Moreover, the calculations reproduced reasonably well the nearly constant behavior of the $B(E2)$ values of ^{114}Te and $^{120-124}\text{Te}$ along the yrast line (Figs. 3 and 4). The constant behavior is related to the competition between the seniority coupling and the neutron-proton correlations. For neutron-deficient Te isotopes, the constant behavior of $B(E2)$ values can be extended to high spin values around $I = 12, 14$, whereas for heavier isotopes, when the neutron-proton correlation gets weaker, the $B(E2)$ values can reduce significantly after $I = 4$ and vanish for the heaviest isotopes.

ACKNOWLEDGMENTS

This work was supported by the Swedish Research Council (VR) under Grants No. 621-2012-3805 and No. 621-2013-4323 and the Göran Gustafsson Foundation. I also thank D. S. Delion for discussions and for his efforts studying above-mentioned nuclei within the coherent state model, and P. Maris for his effort calculating those nuclei with the code MFDn. The computations were performed on resources provided by the Swedish National Infrastructure for Computing (SNIC) at PDC, KTH, Stockholm.

-
- [1] T. Faestermann, M. Gorska, and H. Grawe, *Prog. Part. Nucl. Phys.* **69**, 85 (2013).
- [2] A. Banu *et al.*, *Phys. Rev. C* **72**, 061305(R) (2005).
- [3] A. Corsi *et al.*, *Phys. Lett. B* **743**, 451 (2015).
- [4] J. Cederkäll *et al.*, *Phys. Rev. Lett.* **98**, 172501 (2007).
- [5] G. Cerizza, A. Ayres, K. L. Jones, R. Grzywacz, A. Bey, C. Bingham, L. Cartegni, D. Miller, S. Padgett, T. Baugher, D. Bazin, J. S. Berryman, A. Gade, S. McDaniel, A. Ratkiewicz, A. Shore, S. R. Stroberg, D. Weisshaar, K. Wimmer, R. Winkler, S. D. Pain, K. Y. Chae, J. A. Cizewski, M. E. Howard, and J. A. Tostevin, *Phys. Rev. C* **93**, 021601(R) (2016).
- [6] A. Ekström *et al.*, *Phys. Rev. Lett.* **101**, 012502 (2008).
- [7] P. Doornenbal *et al.*, *Phys. Rev. C* **90**, 061302(R) (2014).
- [8] A. Jungclauss *et al.*, *Phys. Lett. B* **695**, 110 (2011).
- [9] G. Guastalla *et al.*, *Phys. Rev. Lett.* **110**, 172501 (2013).
- [10] J. M. Allmond, A. E. Stuchbery, A. Galindo-Uribarri, E. Padilla-Rodal, D. C. Radford, J. C. Batchelder, C. R. Bingham, M. E. Howard, J. F. Liang, B. Manning, S. D. Pain, N. J. Stone, R. L. Varner, and C.-H. Yu, *Phys. Rev. C* **92**, 041303(R) (2015).
- [11] M. Spieker *et al.*, *Phys. Lett. B* **752**, 102 (2016).
- [12] L. Pellegri *et al.*, *Phys. Rev. C* **92**, 014330 (2015).
- [13] A. Ansari and P. Ring, *Phys. Lett. B* **649**, 128 (2007).
- [14] N. Lo Iudice, C. Stoyanov, and D. Tarpanov, *Phys. Rev. C* **84**, 044314 (2011).
- [15] I. O. Morales, P. Van Isacker, and I. Talmi, *Phys. Lett. B* **703**, 606 (2011).
- [16] H. Jiang, Y. Lei, C. Qi, R. Liotta, R. Wyss, and Y. M. Zhao, *Phys. Rev. C* **89**, 014320 (2014).
- [17] H. Jiang, Y. Lei, G. J. Fu, Y. M. Zhao, and A. Arima, *Phys. Rev. C* **86**, 054304 (2012).
- [18] L. Coraggio, A. Covello, A. Gargano, N. Itaco, and T. T. S. Kuo, *Phys. Rev. C* **91**, 041301 (2015).
- [19] T. Engeland, M. Hjorth-Jensen, M. Kartamyshev, and E. Osnes, *Nucl. Phys. A* **928**, 51 (2014).
- [20] T. Back, C. Qi, B. Cederwall, R. Liotta, F. G. Moradi, A. Johnson, R. Wyss, and R. Wadsworth, *Phys. Rev. C* **87**, 031306 (2013).
- [21] C. Qi and Z. X. Xu, *Phys. Rev. C* **86**, 044323 (2012).
- [22] T. Bäck *et al.*, *Phys. Rev. C* **84**, 041306(R) (2011).
- [23] M. Doncel *et al.*, *Phys. Rev. C* **91**, 061304(R) (2015).
- [24] B. Hadinia *et al.*, *Phys. Rev. C* **72**, 041303(R) (2005).
- [25] E. Caurier, F. Nowacki, A. Poves, and K. Sieja, *Phys. Rev. C* **82**, 064304 (2010).
- [26] Z.-Y. Wu, C. Qi, R. Wyss, and H.-L. Liu, *Phys. Rev. C* **92**, 024306 (2015).
- [27] E. A. Coello Pérez and T. Papenbrock, *Phys. Rev. C* **92**, 064309 (2015).
- [28] Zs. Dombrádi, B. M. Nyakó, G. E. Perez, A. Algora, C. Fahlander, D. Seweryniak, J. Nyberg, A. Atac, B. Cederwall, A. Johnson, A. Kerek, J. Kownacki, L.-O. Norlin, R. Wyss, E. Adamides, E. Ideguchi, R. Julin, S. Juutinen, W. Karczmarczyk, S. Mitarai, M. Piiparinen, R. Schubart, G. Sletten, S. Törmänen, and A. Virtanen, *Phys. Rev. C* **51**, 2394 (1995).

- [29] O. Möller, N. Warr, J. Jolie, A. Dewald, A. Fitzler, A. Linnemann, K. O. Zell, P. E. Garrett, and S. W. Yates, *Phys. Rev. C* **71**, 064324 (2005).
- [30] M. Saxena, R. Kumar, A. Jhingan, S. Mandal, A. Stolarz, A. Banerjee, R. K. Bhowmik, S. Dutt, J. Kaur, V. Kumar, M. Modou Mbaye, V. R. Sharma, and H.-J. Wollersheim, *Phys. Rev. C* **90**, 024316 (2014).
- [31] D. S. Delion, R. Wyss, R. J. Liotta, B. Cederwall, A. Johnson, and M. Sandzelius, *Phys. Rev. C* **82**, 024307 (2010).
- [32] B. Hadinia *et al.*, *Phys. Rev. C* **70**, 064314 (2004).
- [33] M. Sandzelius *et al.*, *Phys. Rev. Lett.* **99**, 022501 (2007).
- [34] D. Seweryniak, K. Starosta, C. N. Davids, S. Gros, A. A. Hecht, N. Hoteling, T. L. Khoo, K. Lagergren, G. Lotay, D. Peterson, A. Robinson, C. Vaman, W. B. Walters, P. J. Woods, and S. Zhu, *Phys. Rev. C* **73**, 061301(R) (2006).
- [35] S. N. Liddick *et al.*, *Phys. Rev. Lett.* **97**, 082501 (2006).
- [36] H. Schatz, A. Aprahamian, V. Barnard, L. Bildsten, A. Cumming, M. Ouellette, T. Rauscher, F.-K. Thielemann, and M. Wiescher, *Phys. Rev. Lett.* **86**, 3471 (2001).
- [37] V.-V. Elomaa *et al.*, *Phys. Rev. Lett.* **102**, 252501 (2009).
- [38] A. J. Boston, E. S. Paul, C. J. Chiara, M. Devlin, D. B. Fossan, S. J. Freeman, D. R. LaFosse, G. J. Lane, M. Leddy, I. Y. Lee, A. O. Macchiavelli, P. J. Nolan, D. G. Sarantites, J. M. Sears, A. T. Semple, J. F. Smith, and K. Starosta, *Phys. Rev. C* **61**, 064305 (2000).
- [39] P. Moeller, R. Bengtsson, B. G. Carlsson, P. Olivius, T. Ichikawa, H. Sagawa, and A. Iwamoto, *At. Data Nucl. Data Tables* **94**, 758 (2008).
- [40] T. Bäck, M. Doncel, B. Cederwall, A. Nyberg, and J. Nyberg, (private communication).
- [41] T. Grahm, *Coulomb Excitation of ^{116}Te and ^{118}Te : A Study of Collectivity above the $Z = 50$ Shell Gap*, CERN-INTC-2015-006;INTC-SR-045 (CERN, Geneva, 2015).
- [42] M. Honma, T. Otsuka, T. Mizusaki, Y. Utsuno, N. Shimizu, and M. Hjorth-Jensen, *RIKEN Accel. Prog. Rep.* **47**, 64 (2014).
- [43] C. B. Hinke *et al.*, *Nature (London)* **486**, 341 (2012).
- [44] D. Seweryniak, M. P. Carpenter, S. Gros, A. A. Hecht, N. Hoteling, R. V. F. Janssens, T. L. Khoo, T. Lauritsen, C. J. Lister, G. Lotay, D. Peterson, A. P. Robinson, W. B. Walters, X. Wang, P. J. Woods, and S. Zhu, *Phys. Rev. Lett.* **99**, 022504 (2007).
- [45] I. G. Darby, R. K. Grzywacz, J. C. Batchelder, C. R. Bingham, L. Cartegni, C. J. Gross, M. Hjorth-Jensen, D. T. Joss, S. N. Liddick, W. Nazarewicz, S. Padgett, R. D. Page, T. Papenbrock, M. M. Rajabali, J. Rotureau, and K. P. Rykaczewski, *Phys. Rev. Lett.* **105**, 162502 (2010).
- [46] R. Machleidt, *Phys. Rev. C* **63**, 024001 (2001).
- [47] M. Hjorth-Jensen, T. T. Kuo, and E. Osnes, *Phys. Rep.* **261**, 125 (1995).
- [48] C. Qi and F. Xu, *Chin. Phys. C* **32**, 112 (2008).
- [49] N. Shimizu, [arXiv:1310.5431](https://arxiv.org/abs/1310.5431).
- [50] Nudat2.6, <http://www.nndc.bnl.gov/nudat2/>.
- [51] R. B. Cakirli, R. F. Casten, J. Jolie, and N. Warr, *Phys. Rev. C* **70**, 047302 (2004).
- [52] D. Hertz-Kintish, L. Zamick, and S. J. Q. Robinson, *Phys. Rev. C* **90**, 034307 (2014).
- [53] I. Talmi, *Simple Models of Complex Nuclei: The Shell Model and Interacting Boson Model* (Harwood Academic, Chur, Switzerland, 1993).
- [54] C. Qi, J. Blomqvist, T. Bäck, B. Cederwall, A. Johnson, R. J. Liotta, and R. Wyss, *Phys. Rev. C* **84**, 021301 (2011).
- [55] Z. X. Xu, C. Qi, J. Blomqvist, R. J. Liotta, and R. Wyss, *Nucl. Phys. A* **877**, 51 (2012).
- [56] B. Cederwall *et al.*, *Nature (London)* **469**, 68 (2011).
- [57] S. Frauendorf and A. Macchiavelli, *Prog. Part. Nucl. Phys.* **78**, 24 (2014).
- [58] C. Qi and R. Wyss, *Phys. Scr.* **91**, 013009 (2016).
- [59] Y. Zhao and A. Arima, *Phys. Rep.* **545**, 1 (2014).
- [60] S. J. Q. Robinson, T. Hoang, L. Zamick, A. Escuderos, and Y. Y. Sharon, *Phys. Rev. C* **89**, 014316 (2014).
- [61] P. Van Iacker, *Int. J. Mod. Phys. E* **22**, 1330028 (2013).